Electronic Supplementary Material (ESI) for Physical Chemistry Chemical Physics.

Anomalous proton conduction behavior across nanoporous two-dimensional conjugated aromatic polymer membrane

Supporting Information

Le Shi*, [a], Zhixuan Ying[a], Ao Xu[b], Yonghong Cheng[a]

a. State key Laboratory of Electrical Insulation and Power Equipment, Center of Nanomaterials for Renewable Energy, School of Electrical Engineering, Xi'an Jiaotong University, Xi'an 710049, China

b. School of Aeronautics, Northwestern Polytechnical University, Xi'an 710072, China

Table S1. Water density and self-diffusion constant at 300 K

	CHON-2017_w	expt.
Water density (g /cm3)	1.00	1.00 [S1]
Self-diffusion constant (Å2/ps)	0.24	0.23 [S2]

Table S2. Calculated proton self-diffusion constant in aqueous environment employing different kinds of density functional and CHON-2017_w ReaxFF.

Density functional	Basis set	Excess proton self-diffusion constant ((Å^2/ps)
BLYP-D3	TZV2P	0.47 [S3]
BLYP	DZVP	0.50 [S3]
BLYP-D3	DZVP	0.62 [S3]
HCTH	DZVP	0.51 [S3]
ReaxFF with CHON-2017_w		1.09 [S4]
Experiment		0.93 [S5]

* Corresponding Author. Email: le.shi@mail.xjtu.edu.cn (Le Shi)

Table S3. Simulation setup for 2D-CAP and G4 in aqueous environment

	a (Å)	b (Å)	c (Å)	N_{water}	ρ_{water}(g/cm^3)
2D-CAP	23.79	34.79	32.53	830	0.922
G4	29.20	25.29	33.08	741	0.906

Table S4. Calculated proton penetration energy barriers across G4 with different simulation time

Simulation time	2 ns	4 ns	6 ns
Energy barrier (kcal·mol^{-1})	2.43	2.62	2.62

Table S5. Calculated proton penetration energy barriers across 2D-CAP with different initial geometries

Initial geometry	Case #1	Case #2	Case #3	Average
Energy barrier (kcal·mol^{-1})	5.53	5.80	5.35	5.56±0.23

Table S6. Calculated proton penetration energy barriers across G4 with different initial geometries

Initial geometry	Case #1	Case #2	Case #3	Average
Energy barrier (kcal·mol^{-1})	2.43	3.01	2.23	2.55±0.41

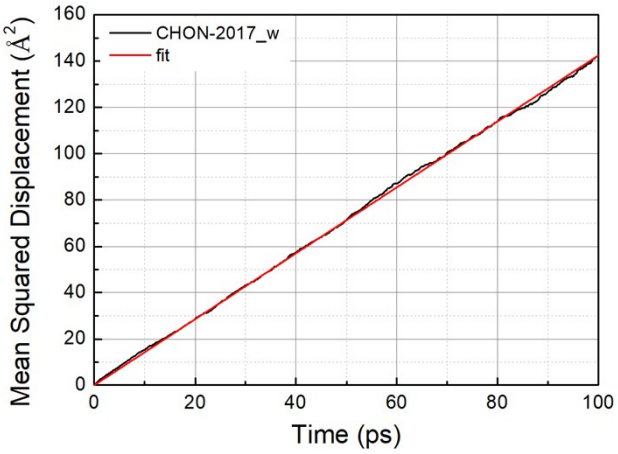

Fig. S1. Predicted and fitted mean square displacement of water as a function of simulation time.

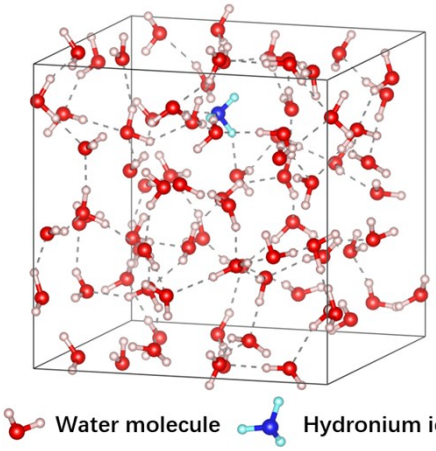

Fig. S2. Simulation setup for proton diffusion in aqueous environment

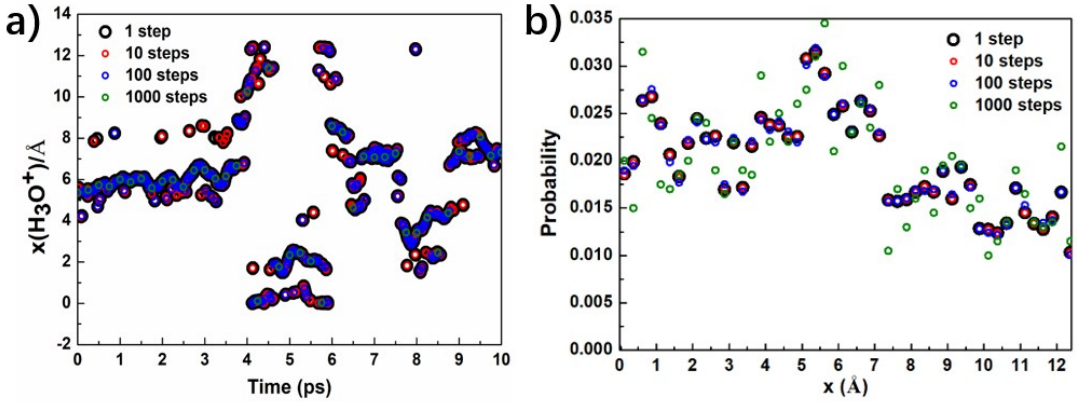

Fig. S3. Influence of sampling rate on (a) obtained proton trajectory and (b) probability distribution for proton position along *x* direction

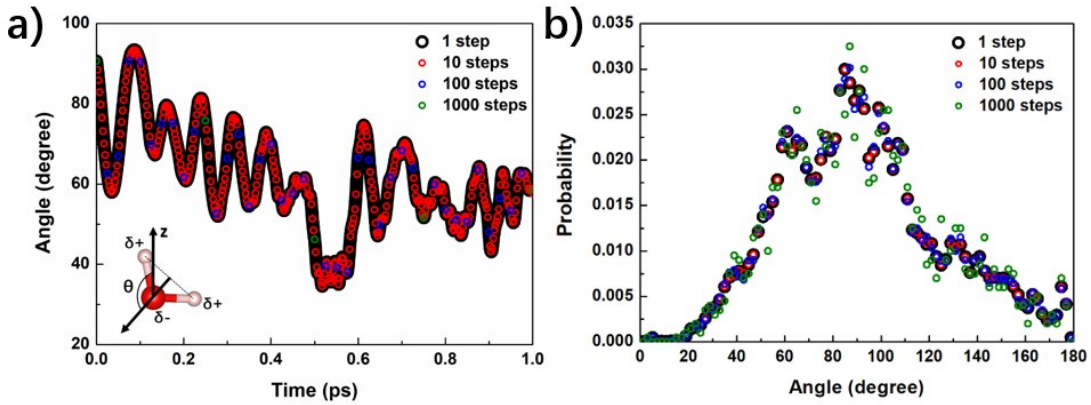

Fig. S4. Influence of sampling rate on (a) obtained water angle and (b) probability distribution of water angle

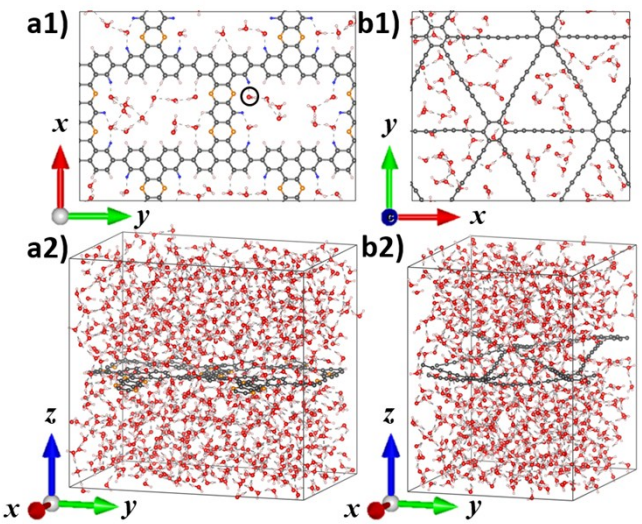

Fig. S5. Snapshot of NVT simulations with 2D materials fully relaxed in aqueous environment.

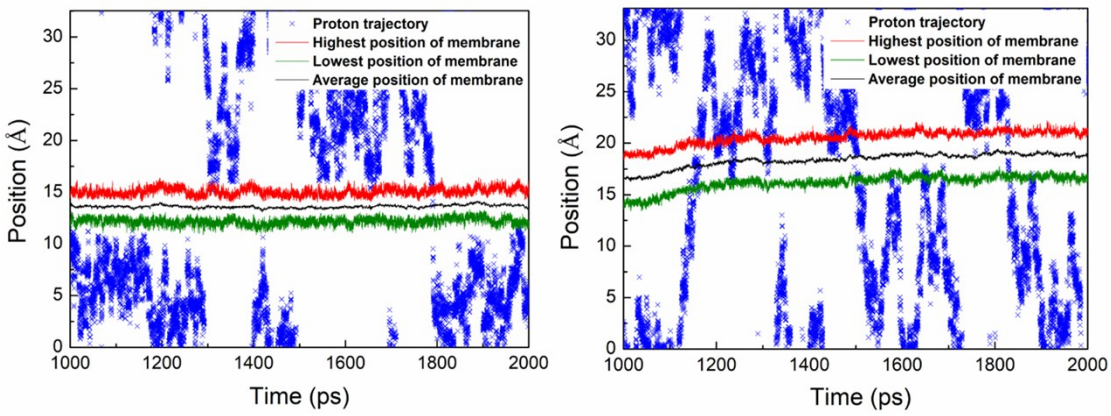

Fig. S6. Distance between proton and (a) 2D-CAP and (b) G4 as a function of simulation time with 2D materials fully relaxed.

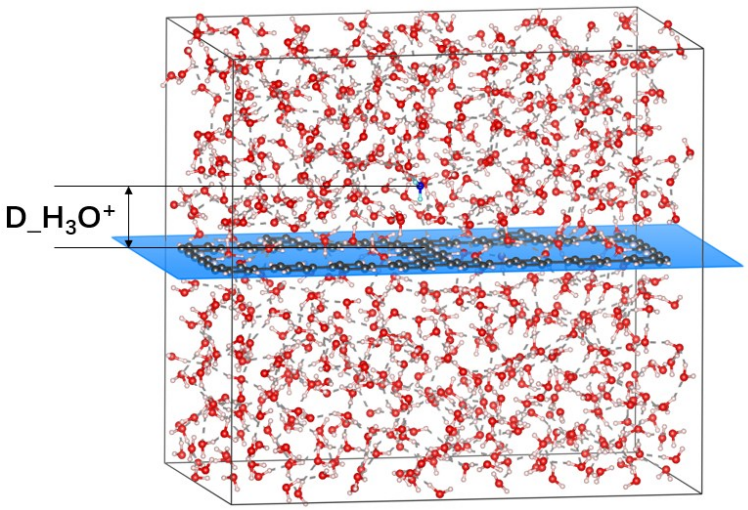

Fig. S7 Metadynamics setup for proton penetration across 2D-CAP.

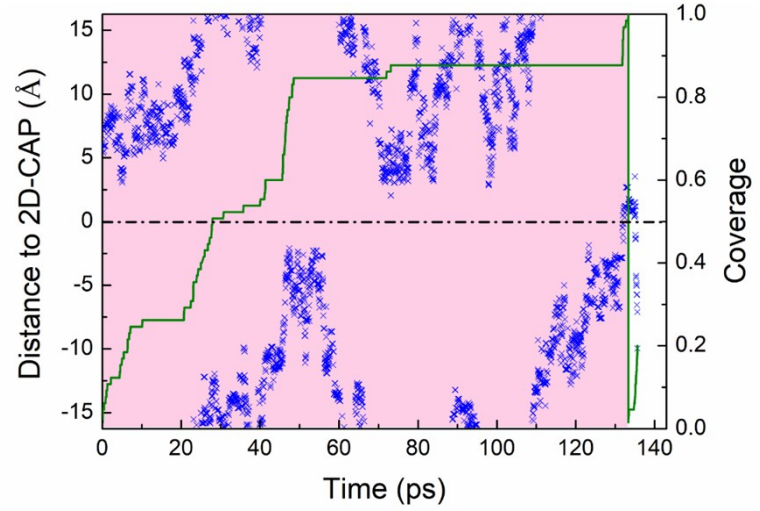

Fig. S8 Distance between proton and 2D-CAP (blue marks) and the coverage of visited proton positions in the phase space (green line) as a function of time in "Case #1" metadynamics simulation of proton penetration. The coverage was reset once it reaches 1. The pink area represents the data used to construct free energy profile.

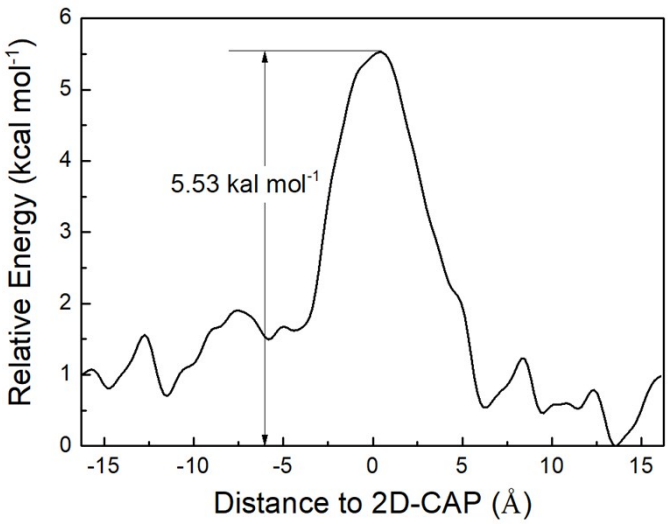

Fig. S9 Free energy profile of proton as a function of the distance to 2D-CAP for "Case #1" metadynamics simulation of proton penetration.

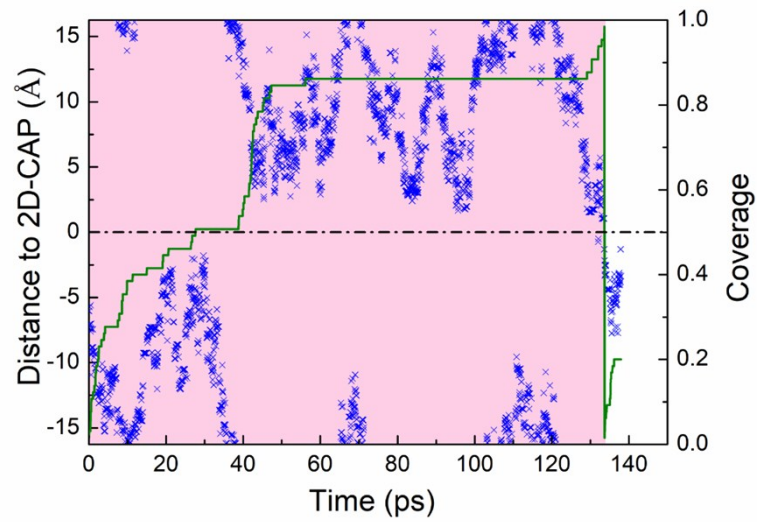

Fig. S10 Distance between proton and 2D-CAP (blue marks) and the coverage of visited proton positions in the phase space (green line) as a function of time in "Case #2" metadynamics simulation of proton penetration. The coverage was reset once it reaches 1. The pink area represents the data used to construct free energy profile.

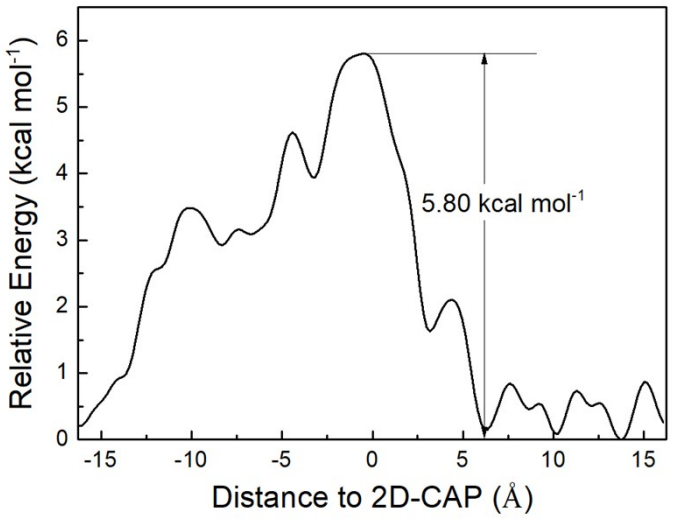

Fig. S11 Free energy profile of proton as a function of the distance to 2D-CAP for "Case #s" metadynamics simulation of proton penetration.

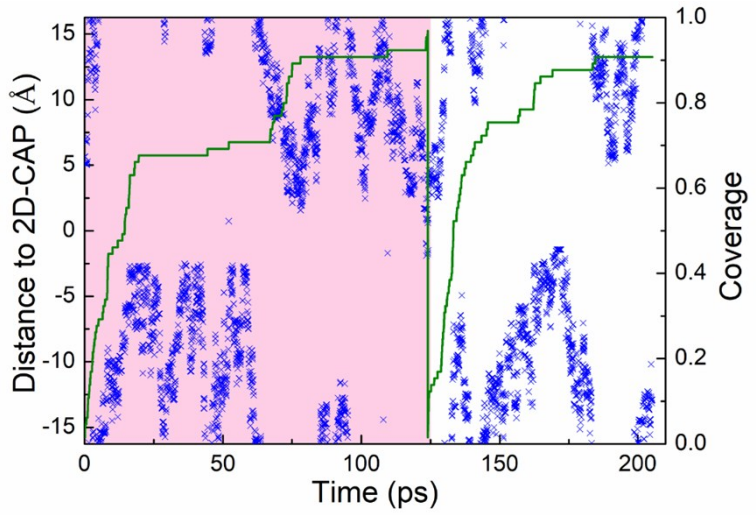

Fig. S12 Distance between proton and 2D-CAP (blue marks) and the coverage of visited proton positions in the phase space (green line) as a function of time in "Case #3" metadynamics simulation of proton penetration. The coverage was reset once it reaches 1. The pink area represents the data used to construct free energy profile.

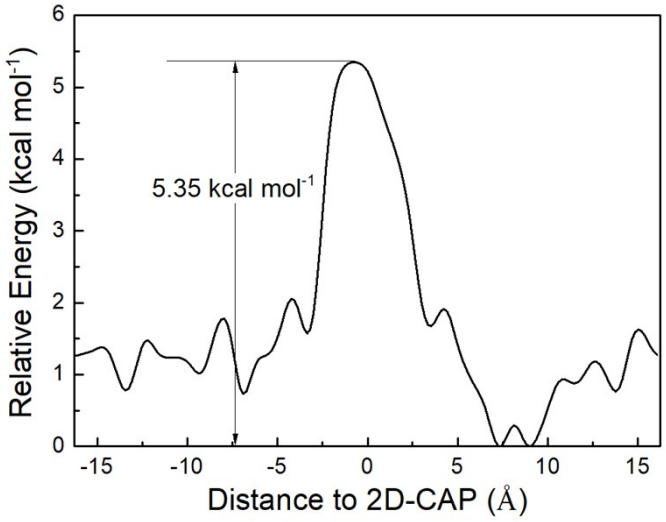

Fig. S13 Free energy profile of proton as a function of the distance to 2D-CAP for "Case #3" metadynamics simulation of proton penetration.

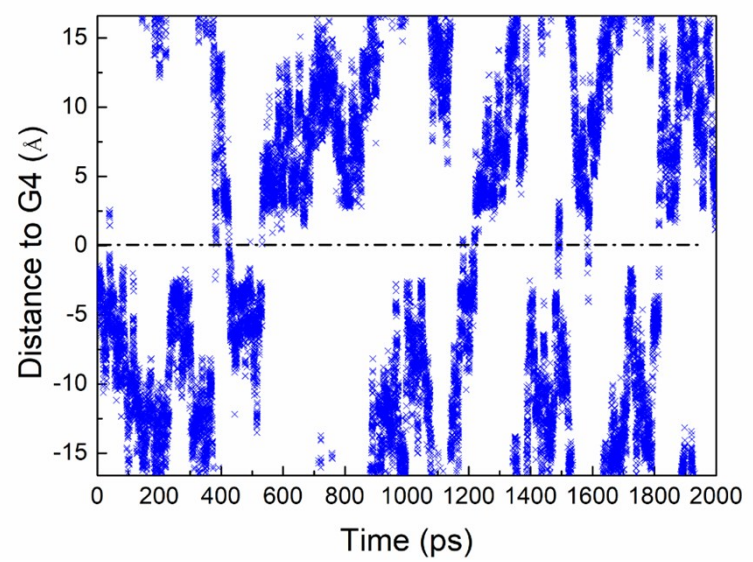

Fig. S14 Distance between proton and G4 (blue marks) as a function of time in "Case #1" MD simulation of proton penetration.

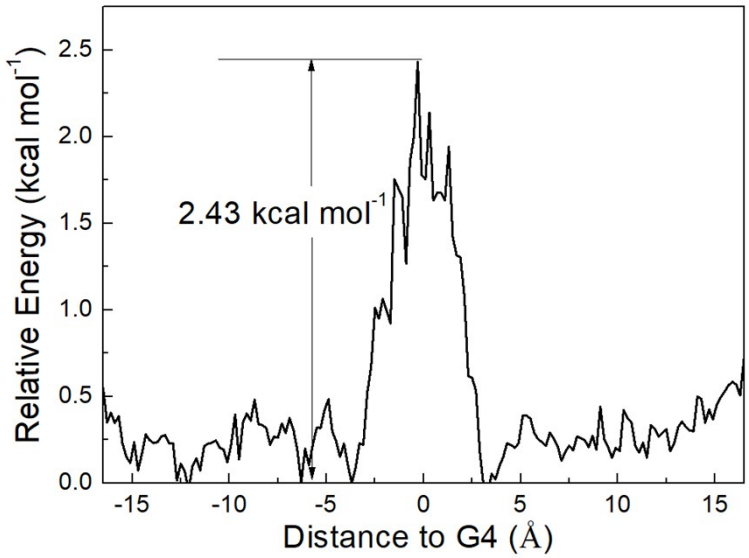

Fig. S15 Free energy profile of proton as a function of the distance to G4 for "Case #1" MD simulation of proton penetration.

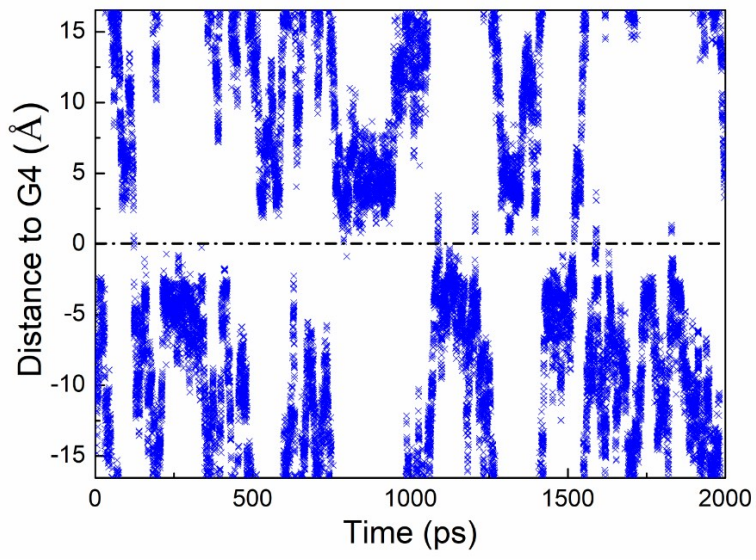

Fig. S16 Distance between proton and G4 (blue marks) as a function of time in "Case #2" MD simulation of proton penetration.

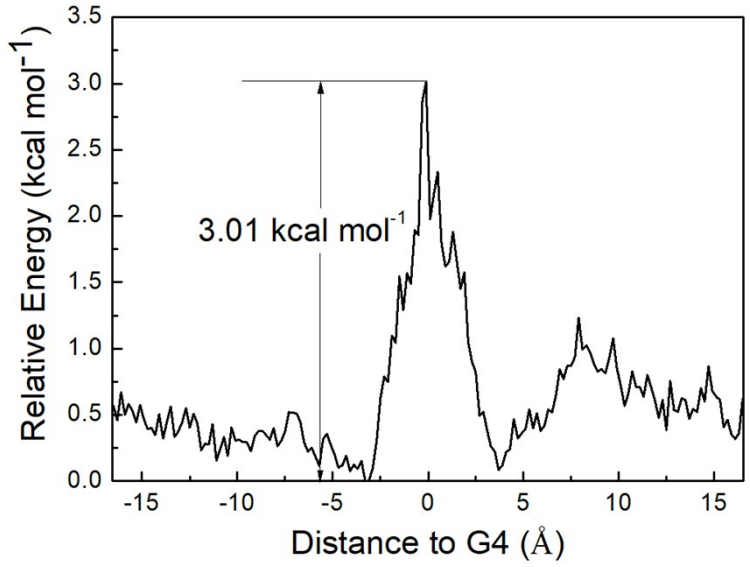

Fig. S17 Free energy profile of proton as a function of the distance to G4 for "Case #2" MD simulation of proton penetration.

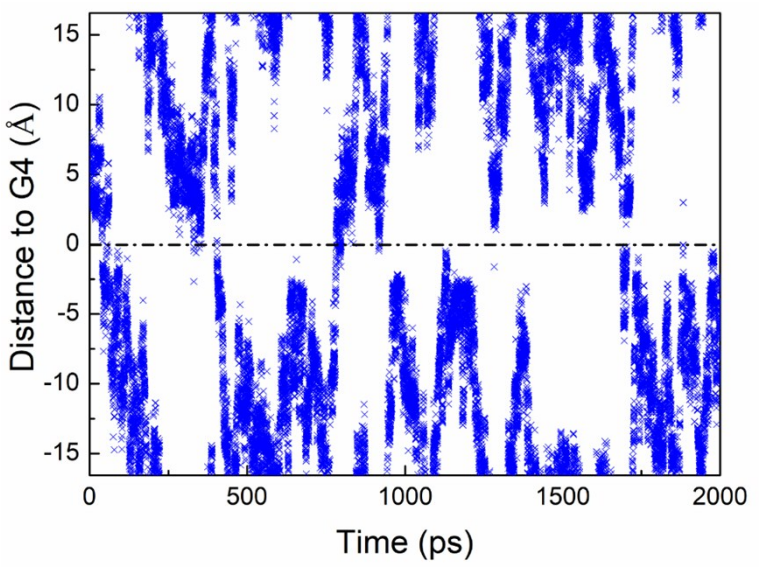

Fig. S18 Distance between proton and G4 (blue marks) as a function of time in "Case #3" MD simulation of proton penetration.

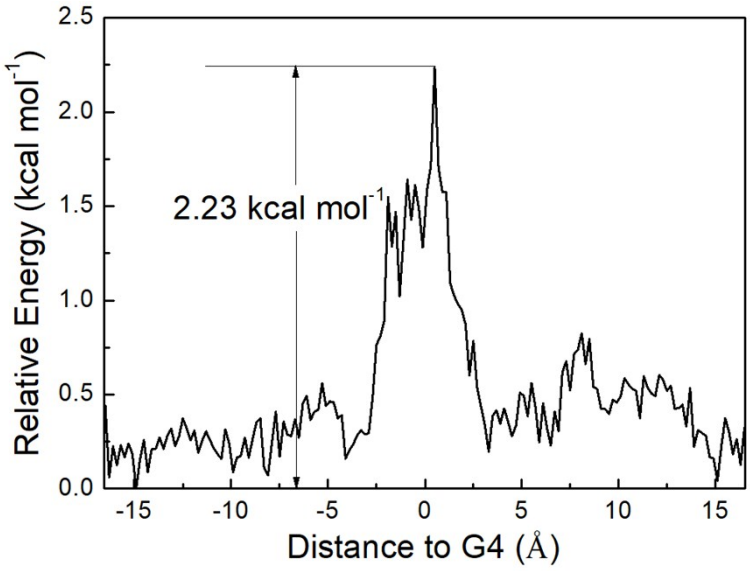

Fig. S19 Free energy profile of proton as a function of the distance to G4 for "Case #3" MD simulation of proton penetration.

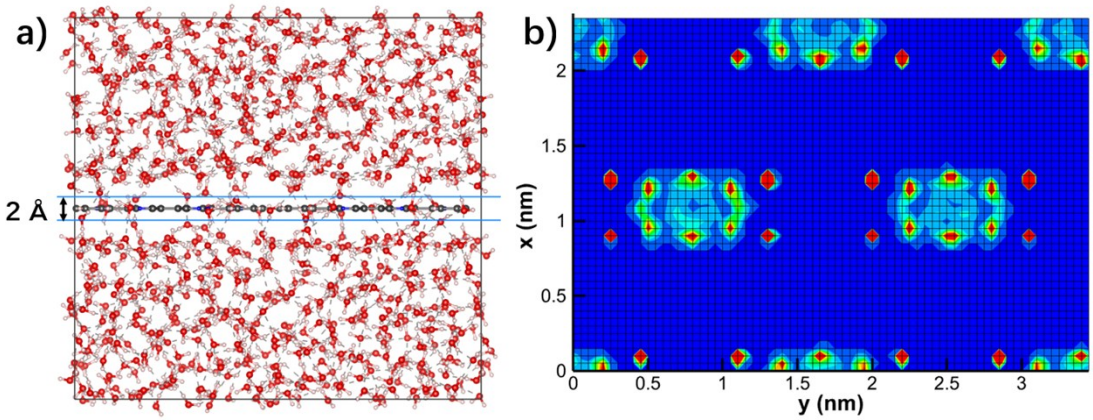

Fig. S20. (a) slab considered when calculating the x-y slice of the time averaged water density (b) mesh grid used when calculating the water density.

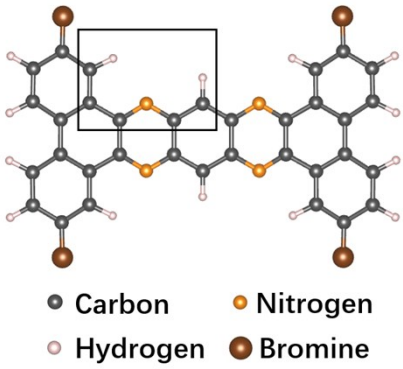

Fig. S21. Atomic structure of the precursor of 2D-CAP

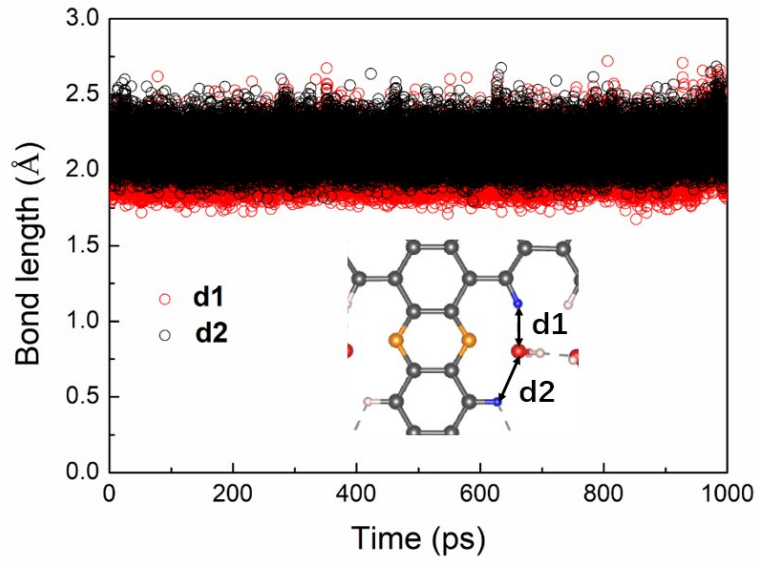

Fig. S22. Distance between the oxygen atom of "anchored water" indicated by black circle in Figure S5(a1) and its nearest H atom in 2D-CAP as a function of simulation

time.

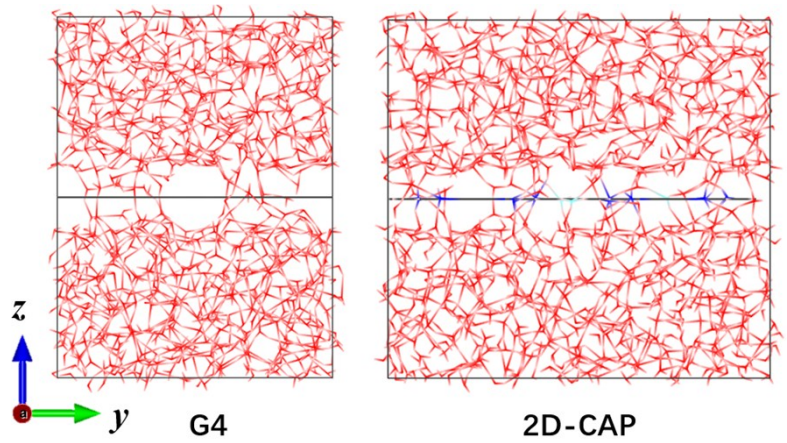

Fig. S23. Water wires penetrating G4 and 2D-CAP. Water molecules bonded to the nanopores were highlighted with blue color

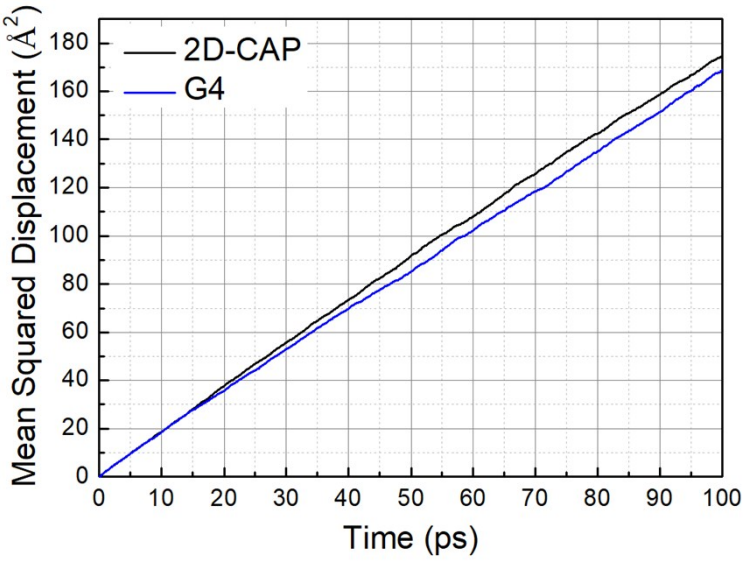

Fig. S24 Mean squared displacement (MSD) of water molecules in both the 2D-CAP and G4 systems as a function of time.

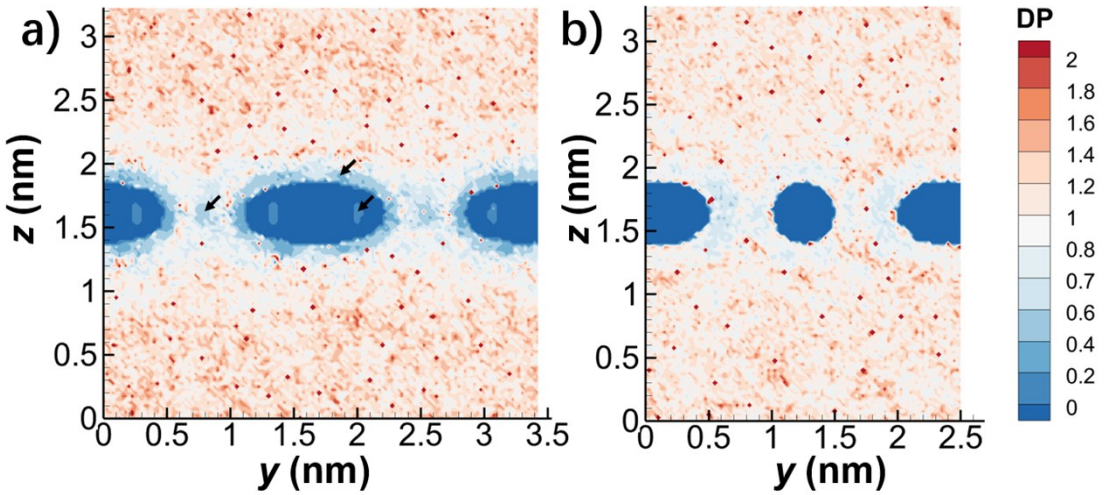

Fig. S25 *y*-*z* slice of the dynamical propensity (t_0=1 ps) at *x* as illustrated in Fig. 5 for (a) 2D-CAP and (b) G4.

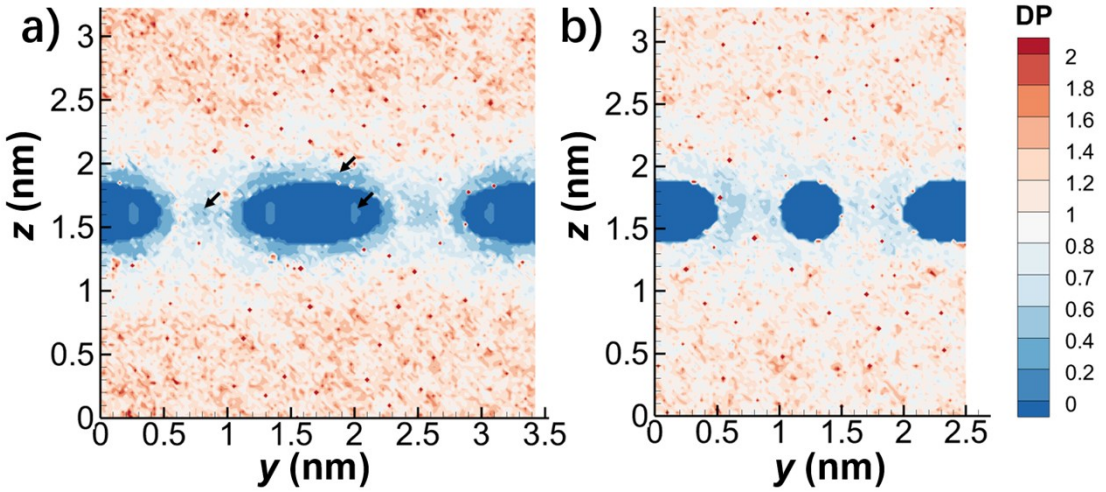

Fig. S26 *y*-*z* slice of the dynamical propensity (t_0=2 ps) at *x* as illustrated in Fig. 5 for (a) 2D-CAP and (b) G4.

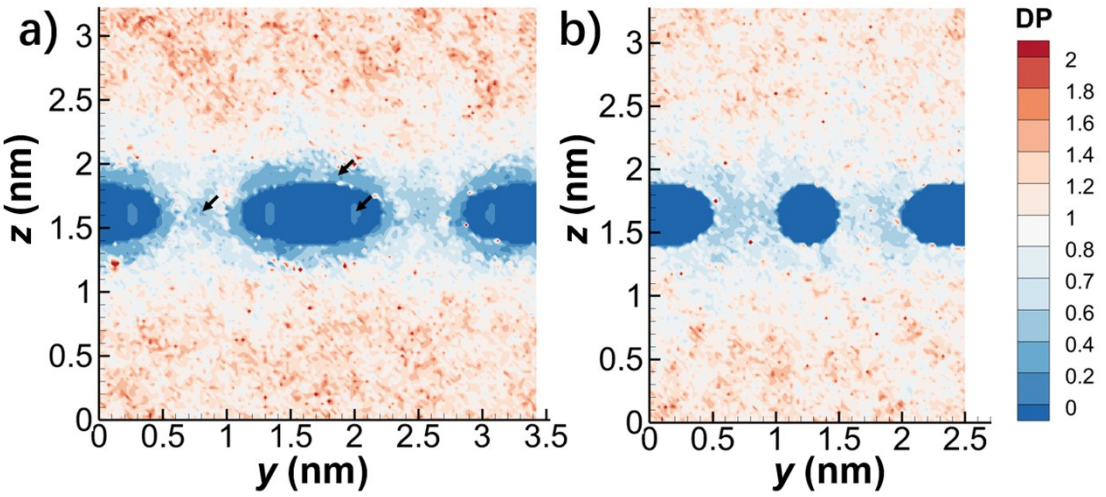

Fig. S27 *y*-*z* slice of the dynamical propensity (t_0=5 ps) at *x* as illustrated in Fig. 5 for (a) 2D-CAP and (b) G4.

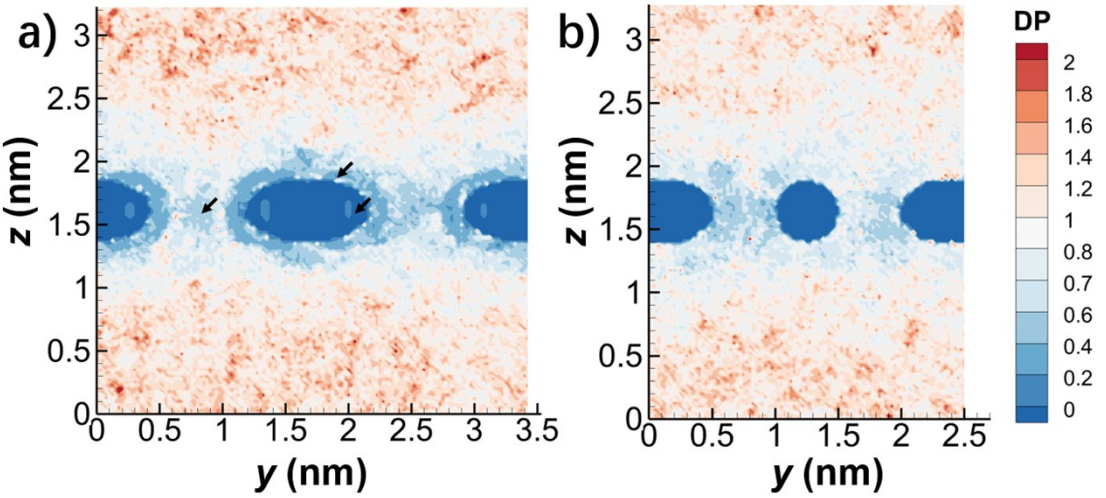

Fig. S28 *y*-*z* slice of the dynamical propensity (t_0=10 ps) at *x* as illustrated in Fig. 5 for (a) 2D-CAP and (b) G4.

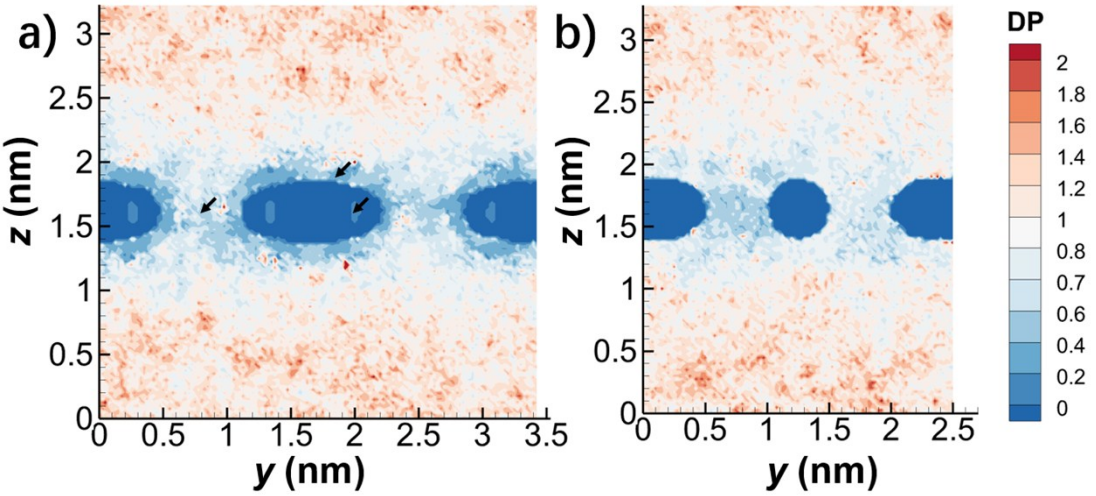

Fig. S29 *y*-*z* slice of the dynamical propensity (t_0=20 ps) at *x* as illustrated in Fig. 5 for (a) 2D-CAP and (b) G4.

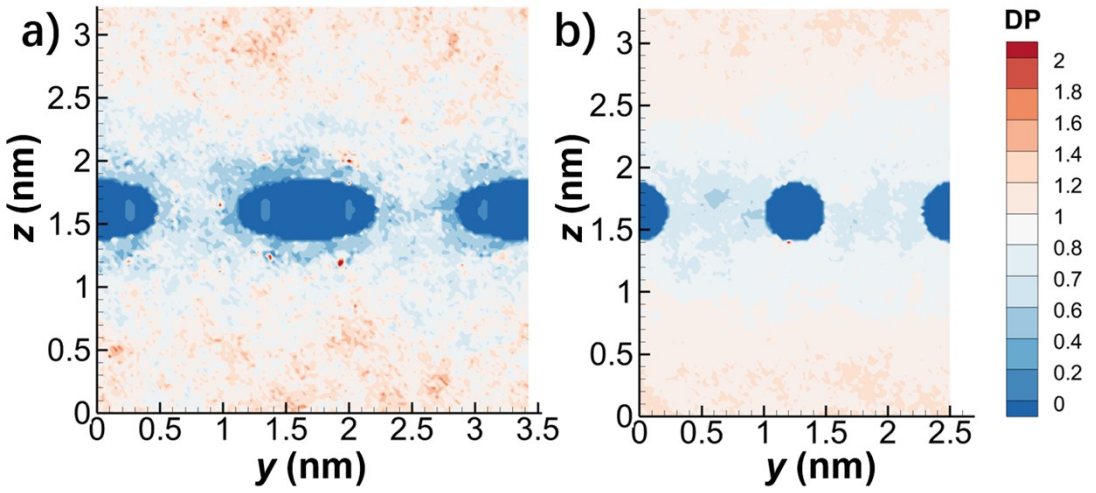

Fig. S30 *y*-*z* slice of the dynamical propensity (t_0=50 ps) at *x* as illustrated in Fig. 5 for (a) 2D-CAP and (b) G4.

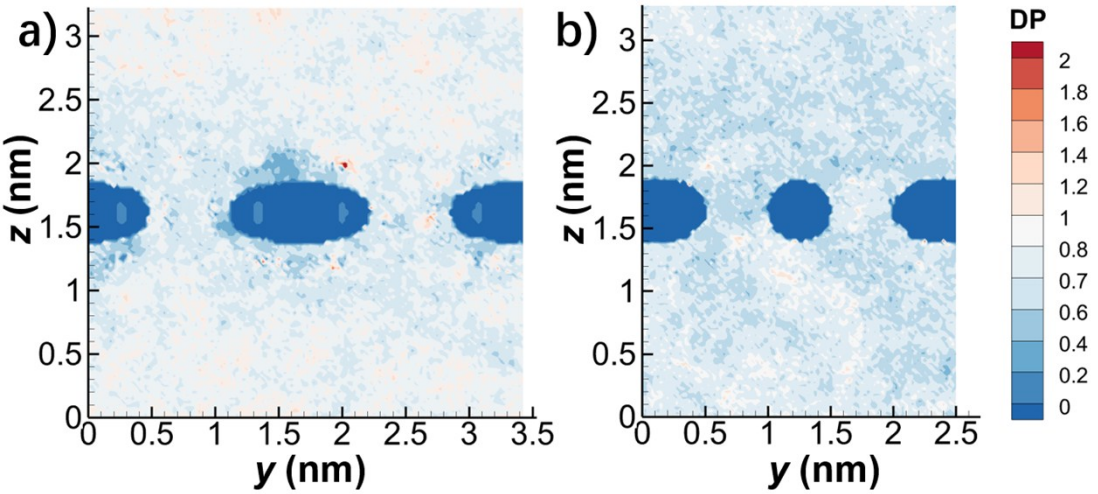

Fig. S31 *y*-*z* slice of the dynamical propensity (t_0=100 ps) at *x* as illustrated in Fig. 5 for (a) 2D-CAP and (b) G4.

References

[S1] W.M. Haynes, T.J. Bruno, D.R. Lide. *CRC Handbook of Chemistry and Physics*, 96th ed., CRC Press: Boca Raton, FL, 2016.

[S2] M. Holz, S.R. Heil, A. Sacco. Temperature-dependent self-diffusion coefficients of water and six selected molecular liquids for calibration in accurate 1H NMR PFG measurements. *Phys. Chem. Chem. Phys.* **2000**, *2(20)*, 4740-2.

[S3] Y.L. Tse, C. Knight, G.A. Voth. An analysis of hydrated proton diffusion in ab initio molecular dynamics. *J. Chem. Phys*. **2015**, *142(1)*, 014104.

[S4] W. Zhang, X. Chen, A.C. Van Duin. Isotope effects in water: Differences of structure, dynamics, spectrum, and proton transport between heavy and light water from ReaxFF reactive force field simulations. *J. Phys. Chem. Lett*. **2018**, *9(18)*, 5445-5452.

[S5] N.K. Roberts, H.L. Northey. Proton and deuteron mobility in normal and heavy water solutions of electrolytes. *J. Chem. Soc. Faraday Trans.* **1974**, *70*, 253-262.